Numerical Study on a Two-Stage Metal Hydride Hydrogen Compression System

Gkanas, E.i.; Grant, D.m.; Stuart, A.d.; Eastwick, C.n.; Book, D.; Nayebossadri, S.; Pickering, L.; Walker, G.s.

DOI:
10.1016/j.jallcom.2015.03.123

Numerical Study on a Two-Stage Metal Hydride Hydrogen Compression System

E.I. Gkanas, D.M. Grant, A.D. Stuart, C.N. Eastwick, D. Book, S. Nayebossadri, L. Pickering, G.S. Walker

PII: S0925-8388(15)00836-1
DOI: http://dx.doi.org/10.1016/j.jallcom.2015.03.123
Reference: JALCOM 33734

To appear in: *Journal of Alloys and Compounds*

Please cite this article as: E.I. Gkanas, D.M. Grant, A.D. Stuart, C.N. Eastwick, D. Book, S. Nayebossadri, L. Pickering, G.S. Walker, Numerical Study on a Two-Stage Metal Hydride Hydrogen Compression System, *Journal of Alloys and Compounds* (2015), doi: http://dx.doi.org/10.1016/j.jallcom.2015.03.123

Numerical Study on a Two-Stage Metal Hydride Hydrogen Compression System

E.I. Gkanas[1], D.M. Grant[1*], A.D. Stuart[1], C. N. Eastwick[1], D. Book[2], S. Nayebossadri[2], L. Pickering[2], G.S. Walker[1]

[1] *Division of Materials, Mechanics and Structures Research Division, Faculty of Engineering, University of Nottingham, Nottingham, NG7 2RD, UK*

[2] *School of Metallurgy and Materials, University of Birmingham, Birmingham, B15 2TT, UK*

Abstract

A multistage metal hydride hydrogen compression (MHHC) system uses a combination of hydride materials in order to increase the total compression ratio, whilst maximizing the hydrogenation rate from the supply pressure at each stage. By solving the coupled heat, mass and momentum conservation equations simultaneously the performance of a MHHC system can be predicted. In the current work a numerical model is proposed to describe the operation of a complete compression cycle. Four different MHHC systems are examined in terms of maximum compression ratio, cycle time and energy consumption and it was found that the maximum compression ratio achieved was 22:1 when operating $LaNi_5$ (AB_5-type) and a Zr-V-Mn-Nb (AB_2-type intermetallic) as the first and second stage alloys respectively in the temperature range of 20 °C (hydrogenation) to 130 °C (dehydrogenation).

Keywords: Metal Hydride Hydrogen Compressor; Metal Hydride; Simulation; Coupled heat and mass transfer; Hydrogenation/Dehydrogenation.

1. Introduction

Hydrogen compression based on the reversible hydrogenation/dehydrogenation ability of metal hydrides has been investigated as a reliable process to compress hydrogen to high pressure without contamination and with low energy costs [1, 2]. A multistage Metal Hydride Hydrogen Compression (MHHC) system uses a combination of different metal hydrides to increase the final compression ratio while maximizing the hydrogenation process from both the supply pressure of each stage. Over the last decade a large number of scientists have made efforts in the subject of MHHC systems and some promising results regarding the material selection and the compression conditions were found both experimentally [3-9] and numerically [10-13]. In most cases, three combinations of materials are selected for a two-stage compression system. The first combination is based on two AB_5-type, usually $LaNi_5$ as the first stage and a $MmNi_{5-y}$-X_y alloy as the second stage yielding a pressure ratio 12:1 when the compressor operates between 20-90 °C [14]. The second case uses an AB_5 material ($LaNi_5$, Ce [15 at.%] + La [Balance]) for the stage 1 and an AB_2 (Ti-Zr-Mn) for the stage 2 [15]. The third typical combination involves two AB_2 intermetallics for stage 1 and stage 2 respectively [16].

The multistage operation approach introduces strict requirements to the tune-ability of the Pressure-Composition-Isotherm (PCI) characteristics, because the coupling of the first stage (dehydrogenation) and the second stage (hydrogenation) requires the plateau pressure (p_{eq}) for the stage 1 metal hydride to be higher than that for stage 2 as shown in Fig.1. Other requirements include: fast kinetics, reduction of compression cycle time; reversibility, high storage capacity to reduce the amount of hydride needed; low plateau slope for the isotherms and low hysteresis. Finally, the cost of the compression process should be affordable [17].

In the current work, a numerical study of a two-stage MHHC is presented. The proposed model was validated with experimental results extracted from a lab scale Sievert-type apparatus and the comparison showed good agreement between the experimental and numerical results. Four different MHHC systems were examined, by using different combinations of materials for the first and second stages, in terms of maximum compression ratio, cycle time and system energy consumption.

2. Model Formulation and Problem Definition

2.1 Introduction of a two-stage MHHC cycle

Fig. 1 illustrates the two-stage compression cycle on a van't Hoff plot, where it is assumed that the temperature range for the stage 1 and stage 2 hydride beds is the same and moves from a low temperature, T_L, up to a high temperature T_H. The compression cycle process is summarized as follows:

Step A: A low pressure hydrogen supply (e.g. an electrolyser) is attached to the first stage, at pressure P_s. The temperature of stage 1 is maintained at T_L, during hydrogenation.

Step B-C: A sensible heating process for the stage 1 metal hydride bed occurs heating the bed to T_H increasing the pressure of the stage 1 vessel.

Step D-E: A coupling process between stage 1 (dehydrogenation at T_H) and stage 2 (hydrogenation at T_L) occurs.

Step F-G: Stage 2 hydride bed undergoes sensible heating in order to achieve the delivery pressure of P_d.

Step H: During dehydrogenation of stage 2 high pressure hydrogen is released from the compressor at P_d.

Fig. 1. A van't Hoff plot illustrating the operation of a two-stage Metal Hydride Hydrogen Compression system from the low temperature T_L to the high temperature T_H. A sensible heating process is performed after each hydrogenation process to increase Peq inside each compression stage. For clarity, the black lines represent the van't Hoff plot for the hydrogenation process for stage 1 (lower black line) and for stage 2 (upper black line).The coupling process between stage 1 and stage 2 is represented by the dashed line.

2.2 Mathematical Model

The following assumptions are made for simplifying the hydrogen storage and compression analysis.

a) Initially the temperature and pressure profiles are uniform.

b) Thermal conductivity and specific heat of the hydrides are assumed to be constant during the compression cycle.

c) The medium is in local thermal equilibrium which implies that there is no heat transfer between solid and gas phases

d) Hydrogen is treated as an ideal gas from a thermodynamic point of view.

2.3 Heat equation

Assuming thermal equilibrium between the hydride powder and hydrogen gas, a single heat equation is solved instead of separate equations for both solid and gas phases:

$$(\rho \cdot Cp)_e \cdot \frac{\partial T}{\partial t} + (\rho_g \cdot Cp_g) \cdot \overline{v}_g \cdot \nabla T = \nabla \cdot (k_e \cdot \nabla T) + m \cdot ((\frac{\Delta \mathrm{H}}{M_{H_2}}) - T \cdot (Cp_g - Cp_s)) \quad (1)$$

Where, the effective heat capacity is given by;

$$(\rho \cdot Cp)_{\mathrm{e}} = \varepsilon \cdot \rho_g \cdot C_{pg} + (1-\varepsilon) \cdot \rho_s \cdot C_{ps} \quad (2)$$

and the effective thermal conductivity is given by;

$$k_e = \varepsilon \cdot k_g + (1-\varepsilon) \cdot k_s \quad (3)$$

The terms ρ_g, C_{pg}, C_{ps} and m refers to the density of the gas phase, the heat capacity of the gas phase, the heat capacity of the solid phase and the kinetic term for the reaction respectively.

2.4 Hydrogen Mass Balance

The equation that describes the diffusion of hydrogen mass inside the metal matrix is given by:

$$\varepsilon \cdot \frac{\partial(\rho_g)}{\partial t} + div(\rho_g \cdot \vec{v}_g) = \pm Q \tag{4}$$

Where, (-) is for the hydrogenation process and (+) is for the dehydrogenation process, v_g is the velocity of gas during diffusion within the metal lattice (see chapter 2.5) and Q is the so-called Mass Source term describing the mass of hydrogen diffused per unit time and unit volume in the metal lattice.

2.5 Momentum equation

The velocity of a gas passing through a porous medium can be expressed by Darcy's law. By neglecting the gravitational effect, the equation which gives the velocity of gas inside the metal matrix is given by:

$$\vec{v}_g = -\frac{K}{\mu_g} \cdot grad(\vec{P}_g) \tag{5}$$

Where K is the permeability of the solid and μ_g is the dynamic viscosity of gas.

2.6 Kinetic expression

The reaction kinetic equation describes the expression for hydrogen mass hydrided and dehydrided per unit time and volume. The amount of hydrogen taken up is given by;

$$m_a = C_a \cdot \exp[-\frac{E_a}{R_g \cdot T}] \cdot \ln[\frac{p_g}{P_{eq}}] \cdot (\rho_{ss} - \rho_s) \tag{6}$$

The amount of hydrogen released from the hydride bed is given by;

$$m_d = C_d \cdot \exp[-\frac{E_d}{R_g \cdot T}] \cdot (\frac{P_{eq} - p_g}{P_{eq}}) \cdot \rho_s \tag{7}$$

Where ρ_s and ρ_{ss} are the density of the hydride at any time and at saturation state respectively. C_{abs} and C_{des} refer to the pre-exponential constants for the hydrogenation and dehydrogenation process and the E_a and E_d are the activation energy for hydrogenation and dehydrogenation process respectively.

2.7 Equilibrium Pressure.

In order to incorporate the effect of hysteresis and the plateau slope (which is present in both stages of the compression cycle) for the calculation of the plateau pressure P_{eq}, the following equation was used [12, 23]:

$$\ln P_{eq} = [\frac{\Delta H}{RT} - \frac{\Delta S}{R} + (\varphi_s \pm \varphi_0) \cdot \tan[\pi \cdot (\frac{x}{x_{sat}} - \frac{1}{2}) \pm \frac{S}{2}] \cdot 10^5 \quad (8)$$

Where φ_s and φ_0 describe the plateau flatness factors and S is the factor which can describe the hysteresis ($\ln P_{abs}/P_{des}$). Furthermore '+' refers for the hydrogenation process, while '-' refers for the dehydrogenation process and x and x_{sat} are the hydrogen concentrations at any given time and at saturation.

3 Results and Discussion

3.1 Material Selection

In the current work, four different cases regarding the material selection of a two-stage MHHC were studied. For stage 1 $LaNi_5$ and $MmNi_{4.6}Al_{0.4}$ were selected and for stage 2 a Zr-V-Mn-Nb AB_2-type intermetallic and a commercially available AB_2-type intermetallic (Hydralloy C5) studied. It should be noted that the use of the stage 1 material requires a higher p_{eq} for the dehydrogenation process than the hydrogenation process of stage 2 material in order to achieve a significant over pressure to charge stage 2 during the coupling process. The materials and the operation temperatures studied are presented in Table 1. The temperature (T_L) for the hydrogenation process was 20 °C for all the cases.

Table 1. MHHC systems used in the current study and the characteristics for a complete compression cycle. The temperature of the hydrogenation process is the same for all the cases T_L=20 °C

The reason that the T_H is higher for Case 1 and Case 3 compared to Case 2 and 4 is that at T_H = 100 °C the value of the p_{eq} for $LaNi_5$ is lower than the p_{eq} for stage 2, while at the same temperature the p_{eq} for $MmNi_{4.6}Al_{0.4}$ is enough to maintain the coupling (see *Section 3.4*).

3.2 Geometry of the System

The schematic of the metal hydride compressor used in the current computational study is shown in Fig. 2. In order to achieve a capacity of 60 g of H_2 per compression cycle the mass of the each hydride required for this study was: 4.45 kg $LaNi_5$, 4.12 kg $MmNi_{4.6}Al_{0.4}$, 3.42 kg Zr-V-Mn-Nb and 3.98 kg Hydralloy C. For simplicity reasons, the porosity of all the hydride beds was chosen to be 0.5, a value which typifies several literature reports [18, 19]. The thermal

management of the tanks for the hydrogenation and dehydrogenation process was achieved by an external jacket, and the thickness of the tank walls was chosen to be 3 mm 316 stainless steel.

Fig. 2. The geometry of the reactors used in the current computational study. A cross-section of the reactor (left) shows that the hydride is inside the reactor and the thickness of the walls of the tank was chosen to be 3mm.The outer diameter of the reactor was 53.8 mm and the length was 378.9 mm. The heating and cooling process is achieved by an external jacket.

3.3 Validation of numerical results

To validate the model, experiments were performed on a 0.8 g sample of $LaNi_5$ powder. The sample was synthesized by arc-melting and phase purity was validated using XRD (Rietveld Analysis). The pressure-composition-isotherm (PCI) hydrogenation and dehydrogenation measurements were performed on a lab scale Sievert-type apparatus with a capacitance manometer (Druck PTX 620) at two different temperatures (25 and 50 ^{o}C). In addition, two different over pressures were used to demonstrate that the model could accommodate different driving pressures. The results of the modeling work compared to the experimental data show good agreement with a maximum deviation less than 5% as illustrated in Fig. 3.

Fig.3. Validation of the predicted amount of hydrogen stored (3a) for different temperatures and different pressures and released (3b) for two different temperatures with experimental data extracted from a lab scale Sievert type apparatus. The experimental results (red dots) with the simulation results (black lines) are in good agreement with a maximum deviation less than 5%.

3.4 Temperature and pressure evolution of a complete two-stage compression cycle.

Fig. 4 shows the bed's average temperature and pressure evolution for the complete two-stage compression cycle with time when using $LaNi_5$ for stage 1 and the AB_2 Zr-V-Mn-Nb intermetallic compound for stage 2 (Case 1). A complete two-stage compression cycle consists of one free hydrogenation process (stage 1), one coupled dehydrogenation (stage 1) - hydrogenation (stage 2) process, a dehydrogenation process (stage 2) and two sensible heating processes (stage 1 and stage 2). For clarity, the two sensible heating processes have not been shown but are represented in Fig. 4 by the vertical dashed line at the end of the first stage hydrogenation process (2000 s) and at the end of the second stage hydrogenation process (4000 s) respectively. However, for the calculation of the total compression cycle time presented in Table 1, the time for the sensible heating process was modelled as 295 s for stage 1 and 276 s for stage 2. During the initial hydrogenation process for stage 1 the exothermic nature of the reaction causes a sudden rise in the bed's temperature, which is followed by a gradual decrease in temperature as the bed is cooled by the external jacket. At the same time, the pressure of

hydrogen within the reactor drops from the initial value of 15 bar supplied from the electrolyser to a final pressure of *ca.* 9 bar, indicating that the hydrogen has been stored inside the metal matrix.

After the hydrogenation process of stage 1, sensible heating takes place raising the temperature inside the reactor from 20 to 130 °C. During the coupling process for case 1, where $LaNi_5$ and AB_2 Zr-V-Mn-Nb are the materials for stage 1 and 2 respectively, the pressure of hydrogen released from stage 1 should be higher than the plateau pressure of stage 2. This is to ensure that there is a large enough overpressure at stage 2 and is ultimately a function of the operating temperature range. For case 1, a sufficiently large over pressure is achieved by the sensible heating process which raises stage 1 to a temperature of 130 ^{o}C resulting in a pressure *ca.* 40 bar, in preparation for the subsequent coupling process.

At the beginning of the coupling there is a maximum pressure difference between the two reactors of 20 bar. During the initial coupling the pressure of stage 1 decreases sharply from 40 bar whilst the pressure of stage 2 increases rapidly from 20 bar. This behavior is due to the fast kinetics between the coupled reactors. After the pressure equalizes across both reactors the continuation of the coupling process results in a gradual increase in pressure until the equilibrium of the driving potential between the two reactors. The insert picture in Fig. 4 describes in detail the above process showing the time needed for the two coupled stages to achieve the initial fast kinetics is 80 s. During the coupling process the temperature of stage 1 rapidly decreases due to the endothermic nature of the dehydrogenation process and then gradually increases towards the temperature of the external jacket. Opposingly, the temperature of stage 2 rapidly increases then gradually decreases towards the temperature of the external jacket. At the end of the coupling process, the pressure of stage 2 is 39 bar and further sensible heating occurs in order to prepare stage 2 for the subsequent dehydrogenation process. The sensible heating process raises the temperature of stage 2 to 130 °C, allowing the final step of the compression cycle to release hydrogen at a pressure of 320-325 bar, yielding a pressure ratio 22:1.

Fig. 4. Bed average Temperature profile (lower part) and Bed average Pressure profile (upper part) for the complete compression cycle of Case 1. The sensible heating proceses are represented by the vertical lines at 2000 s (sensible heating of stage 1) and 4000 s (sensible heating of stage 2). Between 0-2000 s the hydrogenation process of the stage 1 occurs, followed by the sensible heating of stage 1. The coupling process of stage 1 and stage 2 is shown between 2000-4000 followed by the sensible heating of stage 2and finally between 4000-5000 s the high pressure delivery from stage 2 takes place.

3.5 Compression performance of the studied cases

The temperature and pressure profiles of the complete two-stage compression cycle for cases 2,3 and 4 are similar in behaviour to that described previously for case 1 regarding the temperature and pressure curves. However, each case presents advantages and disadvantages when compared to each other.

Case 1 and Case 3 use the same material for stage 1 ($LaNi_5$), but different materials for stage 2. The operation temperature range is the same for both cases (20 – 130 °C), so the energy consumption for the operation of both cases is expected to be almost the same. Case 1 yields higher compression ratio (22:1) compared to Case 3 (20:1) and this difference lies in the different dehydrogenation behaviour of the second stage material for each case. On the other hand, the time for a complete compression cycle is lower for the Case 3, indicating that the second stage material presents faster kinetics comparing to the second stage material for Case 1. Case 2 and Case 4 use the same material for stage 1 ($MmNi_{4.6}Al_{0.4}$) but different materials for stage 2. The operating temperature range (20-100 °C) in both cases is lower compared to Cases 1 and 3, and as a consequence the energy consumption for these cases is significantly lower. The reason for the lower temperature range is that when stage 1 operates at 100 °C at the dehydrogenation process, the pressure is high enough to maintain the coupling process of stage 1 and stage 2. The presence of the Mischmetal at the first stage (~ 50% Ce, ~ 25% La, Nd, Pr) can reduce the unit cell volume and increase the plateau pressure [20-22], so in that way the desired pressure in stage 1 can be achieved at lower temperature. As a consequence for operating at lower temperature the compression ratio of Case 2 and 4 is lower comparing to the previous cases. If the operation temperatures were the same for all cases, the compression ratio would be expected to be almost the same, due to the fact that the materials for the second stage are the same. According to the above analysis, when trying to build a two-stage compression system (or in general a multi-stage compression system), the most important factor in choosing the most suitable materials for the compression stages is the identification of the objectives that the compressor needs to achieve. For example, if the objective is to achieve higher compression ratio and the energy consumption (temperature range) is of minor importance, then the materials and temperature ranges used for Case 1 and 3 are suitable for such application. On the other hand, if the energy consumption is the main concern, then the materials and temperature ranges used for Case 2 and 4 might fulfil the criteria to build the reactor. The ongoing work is to achieve a high compression ratio at the lowest operating temperature range and the lowest cycle time. This will require the further development of materials for stage 1 and stage 2, and improvements in the efficient heat management of the reactors. Another important aspect is the degradation of capacity over long term cycling. This can result in reduction of the capacity and increased plateau slopes. For example, $LaNi_5$ can experience a reduction in capacity of 56% after 520 cycles at 500 K [24]. Improvements can be made by substituting Al or Sn [24, 25]. For example, $LaNi_{4.8}Sn_{0.2}$ only experiences capacity loss of 10% after 1330 cycles at 500 K. This illustrates that degradation through disproportionation and also contamination is an issue that affects candidate hydrides for compressors to different levels. Future work will need to take this into consideration adding a further complexity to the model.

4. Conclusions

A numerical model describing the complete operation of a two-stage hydrogen compression system was presented and analyzed. Four different cases of MHHC systems were studied and compared to each other in terms of compression ratio, cycle time, energy consumption and compression characteristics. It was found that when operating $LaNi_5$ at stage 1 and Zr-V-Mn-Nb (AB_2-type) at stage 2 at a temperature range between 20 °C (hydrogenation) and 130 °C (dehydrogenation) the final compression ratio is 22:1, reaching at the end of the final dehydrogenation process a delivery pressure of 320 bar. For the cases that the first stage material was $MmNi_{4.6}Al_{0.4}$ and the operation of the compressor was between 20 °C and 100 °C the total compression ratio was lower at 12:1 (Case 2) and 11:1 (Case 4) presenting at the end of the dehydrogenation process a delivery pressure of 180 bar, but the cycle time was faster and the energy consumption less.

Acknowledgements

The current work was supported financially by the E.S.C.H.E.R (Engineering Safe and Compact Energy Reserves) Project, EPRSC Reference EP/KO21117/1.

Nomenclature

C_a	*Hydrogenation Constant, s^{-1}*
C_d	*Dehydrogenation Constant, s^{-1}*
C_p	*Specific Heat, J/kg-K*
E	*Activation Energy, $J/molH_2$*
h	*Heat Transfer Coefficient, W/m^2K*
k	*Thermal Conductivity, W/m-K*
K	*Permeability, m^2*
M	*Molecular Weight, kg/mol*
m	*Kinetic Expression*
t	*Time, s*
T	*Temperature, K*
v	*Gas Velocity, m/s*
p	*Pressure, bar*
R	*Gas Global Constant, J/mol-K*

Subscripts

a	*Hydrogenation*
d	*Dehydrogenation*
e	*Effective*
eq	*Equilibrium*
g	*Gas*
s	*Solid*
ss	*Saturation*

Greek Letters

ε	*Porosity*
μ	*Dynamic Viscosity, kg/ms*
ρ	*Density, kg/m^3*
ΔH	*Reaction Enthalpy, J/mol*
ΔS	*Reaction Entropy, J/mol- K*

References

[1] R.C Bowman Jr, J. Alloys Comp., 356-357 (2003) 789-793.

[2] S. Mazumdar, M. Ram Gopal, S Bhattacharyya, Int. J. Hyd. Energy 30 (2005) 631-641.

[3] P. Muthukumar, P. M Maiya, S.S Murthy, Int. J. Hyd. Energy 33 (2008) 463-469.

[4] P. Muthukumar, M.M Prakash, M. Srinivasa, Int. J. Hyd. Energy, 30 (2005) 879-892.

[5] X. Wang, R. Chen, Y. Zhang, C. Changpin, Q. Wang, J. Alloys Comp, 420 (2006) 322-325.

[6] S.S Makridis, E.I Gkanas, G. Panagakos, E.S Kikkinides, A.K Stubos, P. Wagener, S. Barcikowski, Int. J. Hyd. Energy 38 (2013) 11530-11535.

[7] H. Li, X. Wang, X. Dong, L. Xu, C. Chen, J. Alloys Comp, 502 (2010) 503-507.

[8] P. Muthukumar, M. Linder, R. Mertz, E. Laurien, Int. J. Hyd. Energy 34 (2009)1873-1879.

[9] E.D Koultoukis, E.I. Gkanas, S.S. Makridis, C.N Christodoulou, D. Fruchard, A.K Stubos, Int. J. Energy Research 38 (2014) 477-486.

[10] E.I Gkanas, S.S Makridis, A.K Stubos, Computer Aided Chem. Eng., 32 (2013) 379-384.

[11] Y. Wang, F. Yang, X. Meng, Q. Guo, Z. Zhang, I.S Park, S. Kim, K.J Kim, Int. J. Hyd. Energy, 35 (2010) 321-328.

[12] P. Muthukumar, K.S Patel, P. Sachan, N. Singhal, Int. J. Hyd. Energy, 37 (2012) 3797-3806.

[13] B.A Talaganis, G.O Meyer, P.A Aguirre, Int. J. Hyd. Energy, 36 (2011) 13621-13631.

[14] R.R Hopkins, K.J Kim, Int. J. Hyd. Energy, 35 (2010) 5693-5702.

[15] M. Lototskyy, Ye. Klochko, V. Linkov, P. Lawrie, B.G. Pollet, Energy Procedia, 29 (2012) 347-356.

[16] X. Wang, H. Liu, H. Li, Int. J. Hyd. Energy, 36 (2011) 9079-9085

[17] M.V. Lototskyy, V.A. Yartys, B.G. Pollet, R.C. Bowman Jr, Int. J. Hyd. Energy, 39 (2014) 5818-5851.

[18] J. Nam, J. Ko, H. Ju, Th. Energy Management in the Process Industries, 89 (2012) 164-175.

[19] M. Raju, S. Kumar, Int. J. Hyd. Energy, 36 (2011) 1578-1591.

[20] T. Kodama, J. Alloys Comp., 289 (1999) 207-212.

[21] E. Anil Kumar, M. Prakash Maiya, S. Srinivas Murthy, J. Alloys Comp., 470 (2009) 157-162.

[22] J. Chen, S.X Dou, H.K. Liu, J. Power Sources, 63 (1996) 267-270.

[23] T. Nashizaki, K. Miyamoto, J. Less Common Metals, 89 (1983) 559-566

[24] R.C Bowman Jr, C.H Luo, C.C Ahn, C.K Witham, B. Fultz, J. Alloys Comp., 217 (1995) 185-192.

[25] E.M Borzone, M.V Blanco, G.O Mayer, A. Baruj, Int. J. Hyd. Energy, 39 (2014) 10517-10524.

Figure Caption List

Fig. 1. A van't Hoff plot illustrating the operation of a two-stage Metal Hydride Hydrogen Compression system from the low temperature T_L to the high temperature T_H. A sensible heating process is performed after each hydrogenation process to increase Peq inside each compression stage. For clarity, the black lines represent the van't Hoff plot for the hydrogenation process for stage 1 (lower black line) and for stage 2 (upper black line).The coupling process between stage 1 and stage 2 is represented by the dashed line.

Fig. 2. The geometry of the reactors used in the current computational study. A cross-section of the reactor (left) shows that the hydride is inside the reactor and the thickness of the walls of the tank was chosen to be 3mm.The outer diameter of the reactor was 53.8 mm and the length was 378.9 mm. The heating and cooling process is achieved by an external jacket.

Fig.3. Validation of the predicted amount of hydrogen stored (3a) for different temperatures and different pressures and released (3b) for two different temperatures with experimental data extracted from a lab scale Sievert type apparatus. The experimental results (red dots) with the simulation results (black lines) are in good agreement with a maximum deviation less than 5%.

Fig. 4. Bed average Temperature profile (lower part) and Bed average Pressure profile (upper part) for the complete compression cycle of Case 1. The sensible heating proceses are represented by the vertical lines at 2000 s (sensible heating of stage 1) and 4000 s (sensible heating of stage 2). Between 0-2000 s the hydrogenation process of the stage 1 occurs, followed by the sensible heating of stage 1. The coupling process of stage 1 and stage 2 is shown between 2000-4000 followed by the sensible heating of stage 2and finally between 4000-5000 s the high pressure delivery from stage 2 takes place.

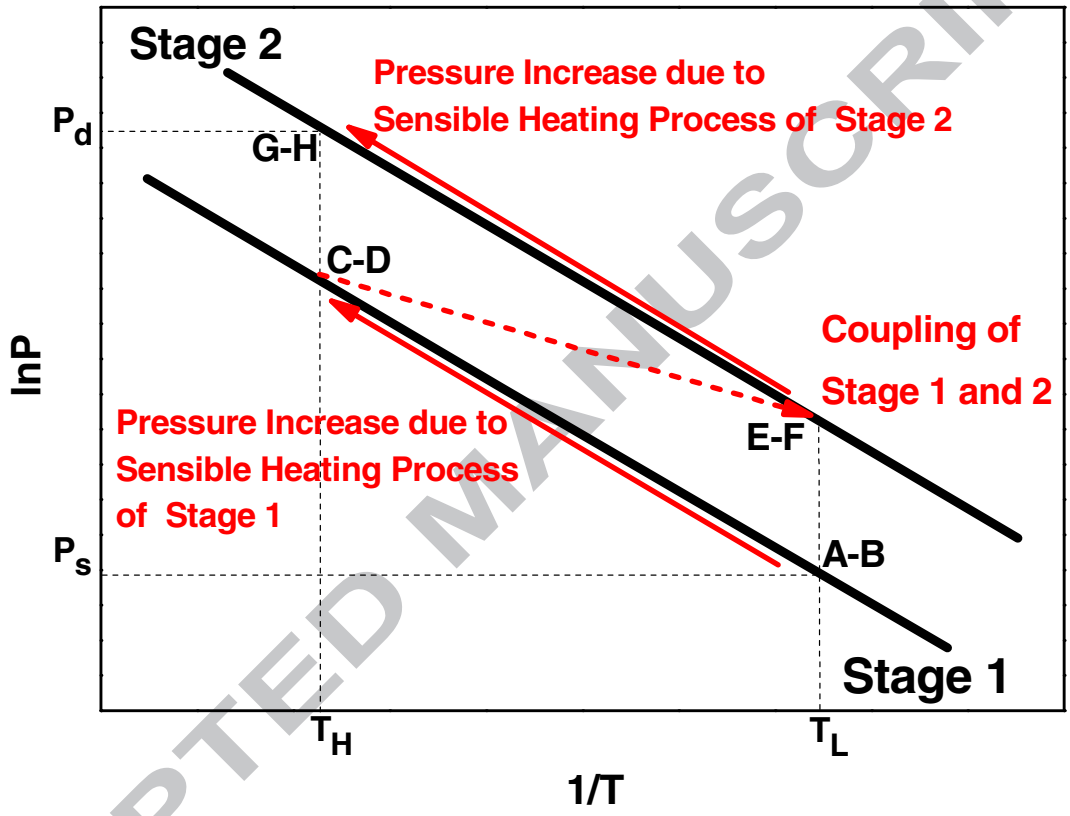

Fig. 1. A van't Hoff plot illustrating the operation of a two-stage Metal Hydride Hydrogen Compression system from the low temperature T_L to the high temperature T_H. A sensible heating process is performed after each hydrogenation process to increase Peq inside each compression stage. For clarity, the black lines represent the van't Hoff plot for the hydrogenation process for stage 1 (lower black line) and for stage 2 (upper black line).The coupling process between stage 1 and stage 2 is represented by the dashed line.

.

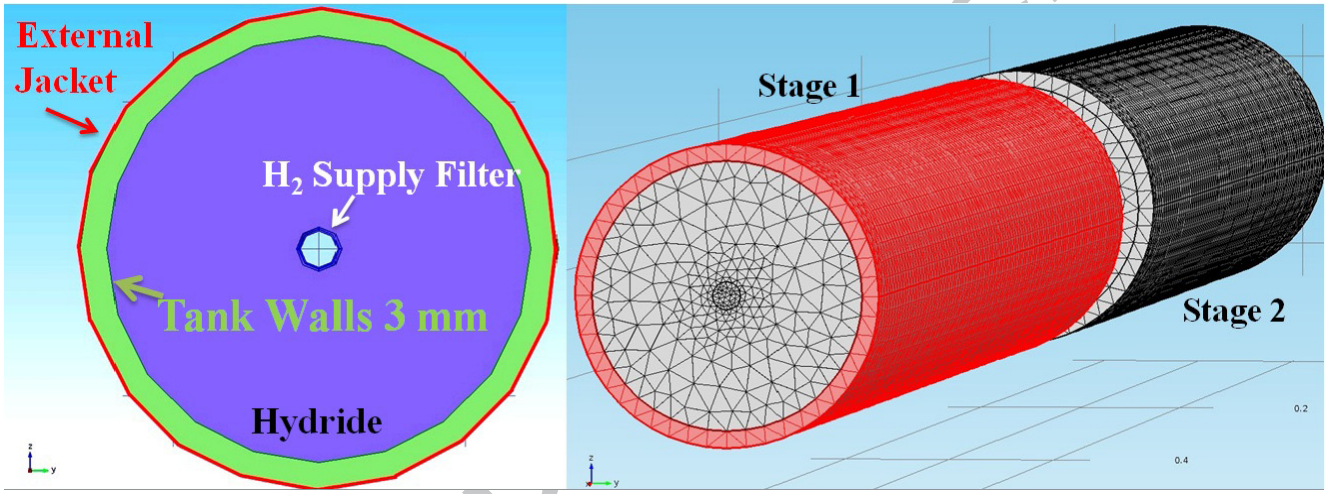

Fig. 2. The geometry of the reactors used in the current computational study. A cross-section of the reactor (left) shows that the hydride is inside the reactor and the thickness of the walls of the tank was chosen to be 3mm.The outer diameter of the reactor was 53.8 mm and the length was 378.9 mm. The heating and cooling process is achieved by an external jacket

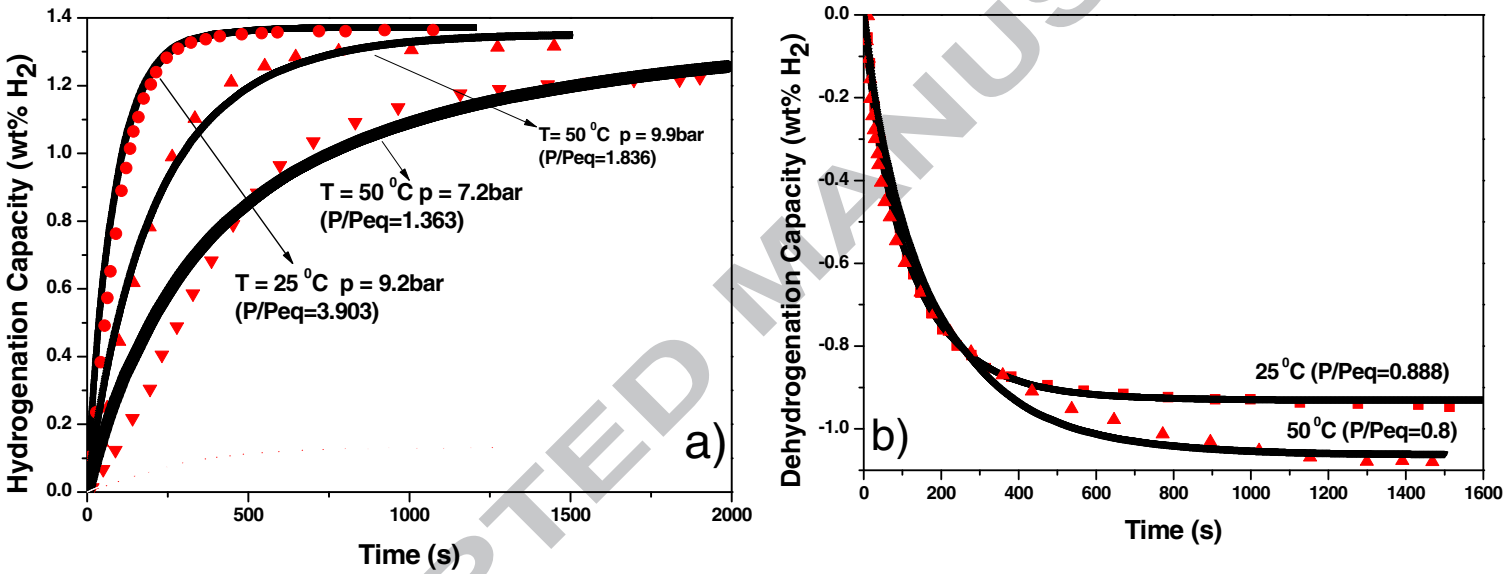

Fig.3. Validation of the predicted amount of hydrogen stored (3a) for different temperatures and different pressures and released (3b) for two different temperatures with experimental data extracted from a lab scale Sievert type apparatus. The experimental results (red dots) with the simulation results (black lines) are in good agreement with a maximum deviation less than 5%.

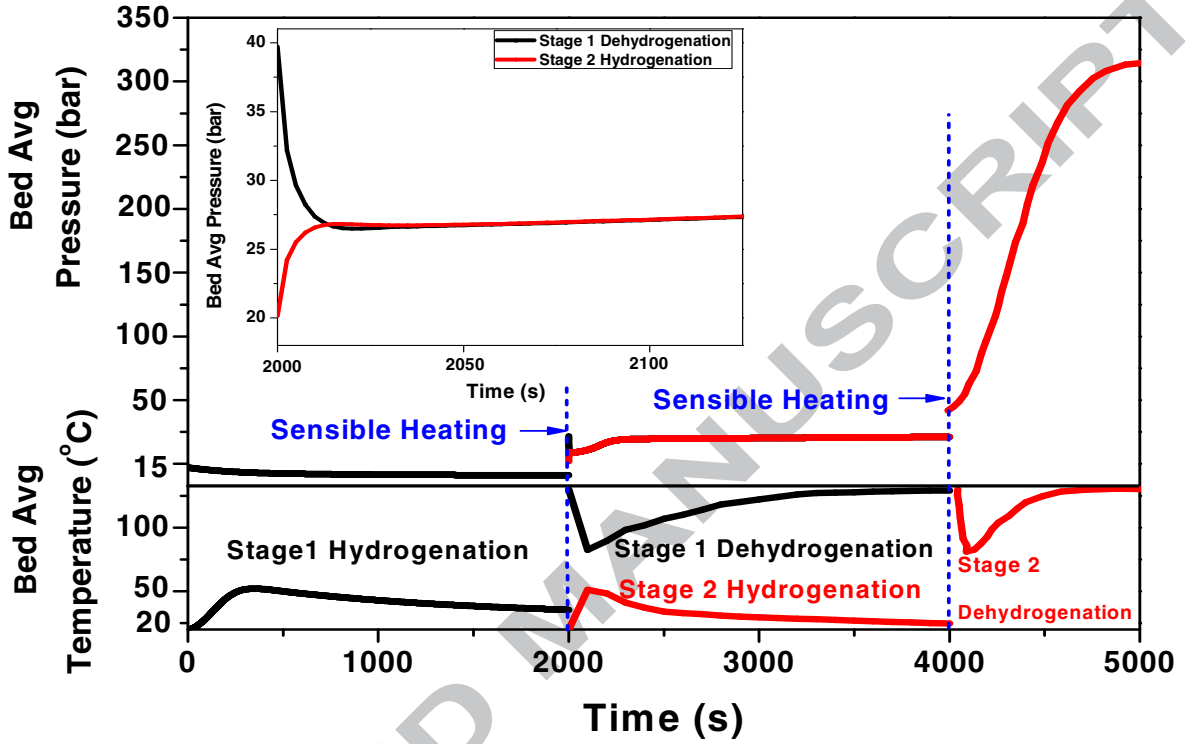

Fig. 4. Bed average Temperature profile (lower part) and Bed average Pressure profile (upper part) for the complete compression cycle of Case 1. The sensible heating proceses are represented by the vertical lines at 2000 s (sensible heating of stage 1) and 4000 s (sensible heating of stage 2). Between 0-2000 s the hydrogenation process of the stage 1 occurs, followed by the sensible heating of stage 1. The coupling process of stage 1 and stage 2 is shown between 2000-4000 followed by the sensible heating of stage 2and finally between 4000-5000 s the high pressure delivery from stage 2 takes place.

Table 1. MHHC systems used in the current study and the characteristics for a complete compression cycle. The temperature of the hydrogenation process is the same for all the cases T_L=20 °C

	First Stage (AB_5)	Second Stage (AB_2)	T_H(°C)	Cycle Time	Compression Ratio	Energy Consumption
Case 1	**$LaNi_5$**	**Zr-V-Mn-Nb**	**130**	**78-80 min**	**22:1**	**10-11 kJ**
Case 2	**$MmNi_{4.6}Al_{0.4}$**	**Zr-V-Mn-Nb**	**100**	**65-67 min**	**12:1**	**8 kJ**
Case 3	**$LaNi_5$**	**Ti-Zr-V-Fe-Cr-Mn**	**130**	**70-72 min**	**20:1**	**10-11 kJ**
Case 4	**$MmNi_{4.6}Al_{0.4}$**	**Ti-Zr-V-Fe-Cr-Mn**	**100**	**63-65 min**	**11:1**	**8-9 kJ**

Highlights:

- Simulation Study of a two-stage Metal Hydride Hydrogen Compression (MHHC) System
- Comparison of Four Different Compression Systems
- Maximum Pressure Ratio 22:1
- Maximum Delivery Pressure 320 bar at 130 ^{o}C